



# Modelling of strongly swirling flows in a complex geometry using unstructured meshes

Junye Wang

*Department of Aeronautical and Automotive Engineering,  
Loughborough University, Loughborough, UK, and*

Geoffrey H. Priestman and John R. Tippetts

*Department of Chemical and Process Engineering, University of Sheffield,  
Sheffield, UK*

## Abstract

**Purpose** – Seeks to examine the performance of conventional turbulence models modelling strongly swirling flows within a Symmetrical Turn up Vortex Amplifier, with adjustment of the turbulence model constants to improve agreement with experimental data.

**Design/methodology/approach** – First, the standard  $k-\varepsilon$  model and the Reynolds Stress Model (RSM) were used with standard values of model constants, using both the first order upwind and the quadratic upstream interpolation for convective kinetics (QUICK) schemes. Then, the swirling effect was corrected by adjusting the model coefficients.

**Findings** – The standard RSM with the QUICK did produce better predictions but still significantly overestimated the experimental data. Much improved simulation was obtained with the systematic adjustment of the model constants in the standard  $k-\varepsilon$  model using the QUICK. The physical significance of the model constants accounted for changes of the eddy viscosity, and the production and destruction of  $k$  and  $\varepsilon$ .

**Research limitations/implications** – More industrial cases could benefit from this simple and useful approach.

**Originality/value** – The constant adjustment is regular and directed, based on the eddy viscosity and the production and destruction of  $k$  and  $\varepsilon$ . The regularity of the effect of the model constants on the solutions makes it easier to quickly adjust them for other industrial applications.

**Keywords** Flow, Fluidics, Turbulence, Modelling, Simulation

**Paper type** Research paper

## Nomenclature

$C_{\mu}, C_1,$   
 $C_2, C_{1\varepsilon},$   
 $C_{2\varepsilon}, C_3$  = constants in turbulence model  
 $k$  = turbulent kinetic energy  $\text{m}^2/\text{s}^2$   
 $Pr_i$  = Prandtl number for energy  
 $u_i$  = mean velocity in direction  $x_i$  m/s  
 $u_j$  = mean velocity in direction  $x_j$   
 $\rho u_i' u_j'$  = Reynolds stress  
 $x_i, x_j$  = coordinate  
 $y$  = the normal distance from the wall  
 at the cell centres

$y^+$  = a distance from the wall at the wall-adjacent cells, defined as  $\rho u_i y / \mu$

## Greek letters

$\beta$  = coefficient of thermal expansion  
 $\varepsilon$  = turbulent dissipation rate,  $\text{m}^2/\text{s}^3$   
 $\mu$  = dynamic viscosity,  $\text{Pa}\cdot\text{s}$   
 $\mu_t$  = turbulent viscosity (defined by equation (3))



---

$\rho$  = density, kg/m<sup>3</sup>  
 $\sigma_k, \sigma_\epsilon$  = constants

$\delta_{ij}$  = Kronecker symbol,  $\delta_{ij} = 1$  if  $i = j$   
and  $\delta_{ij} = 0$  if  $i \neq j$

## 1. Introduction

The vortex amplifier is a generic fluidic component which has been used in many varied applications ranging from ventilation flow control to flow measurement (Wang *et al.*, 1997; Priestman and Tippetts, 1984). The turn-up vortex amplifier or TuVA is a type of vortex amplifier in which a supply and a control flow both enter a vortex chamber periphery tangentially, but in opposition, such that the introduction of control flow tends to oppose the vortex created by the supply flow, with the result that the through-flow is increased or “turned-up”. The control inlet is normally relatively small, such that a relatively high pressure but low flow control stream modulates a much larger but lower pressure supply flow. The Symmetrical Turn-up Vortex Amplifier (STuVA), is a special design of TuVA in which the control and supply ports are identical to each other, giving symmetry to the device. The STuVA has unique and complex characteristics. A common pressure supplied to the control and supply ports give a maximum through-flow with, in theory, no vortex, whilst a minimum through-flow and maximum vortex strength is achieved if flow only enters through one of the inlet ports. These special characteristics enable the STuVA to be applied as a level control in pressurised vessels, such as oil-gas production separators (Priestman and Tippetts, 1998, 2000, 2002).

It was found that a basic two inlet port STuVA exhibited an internal flow instability when applied in a level control system (Priestman and Tippetts, 2000). The problem was found to be associated with an inability of the device to establish a completely vortex free flow state in the maximum flow condition. It was found, however, that the problem could be avoided if the supply and control flows were divided between multiple chamber inlets, as illustrated in the eight port STuVA design shown in Figure 1.

The STuVA operating characteristics are quite complex, but in applications such as level control, its performance is mainly determined by its two extreme operating states: the maximum flow no vortex state and the minimum flow high vortex state. Previous works (Priestman and Tippetts, 1998, 2000) has concentrated on experimental optimisation of the flow ratio of these states by changing the STuVA geometry and measuring its performance. Uncertainty remains, however, over several important design criteria, such as the scaling, cavitation and stability, with currently a lack of theoretical understanding of fluid flow within the device. However, numerical analysis is difficult because the complex flows include impingement, strong swirling, strong acceleration and internal recirculation. With the rapid advances of computer technology and numerical methods, it becomes possible to apply computational fluid dynamics (CFD) directly to tackle such a complex design problem.

A recent study of non-swirling flow within the STuVA (Wang *et al.*, n.d.), used three turbulent models, the standard  $k-\epsilon$  model, the  $k-\epsilon$  RNG, and the Reynolds Stress Model (RSM) with the standard model constants, and three types of near-wall treatments. Most combinations gave reasonable predictions, however, it was found that the RSM, two layer wall model and the quadratic upstream interpolation for convective kinetics (QUICK) scheme produced better performance than other model combinations for the non-swirling flows. However, it has not been confirmed if this combination can also produce a better performance for strongly swirling flows.

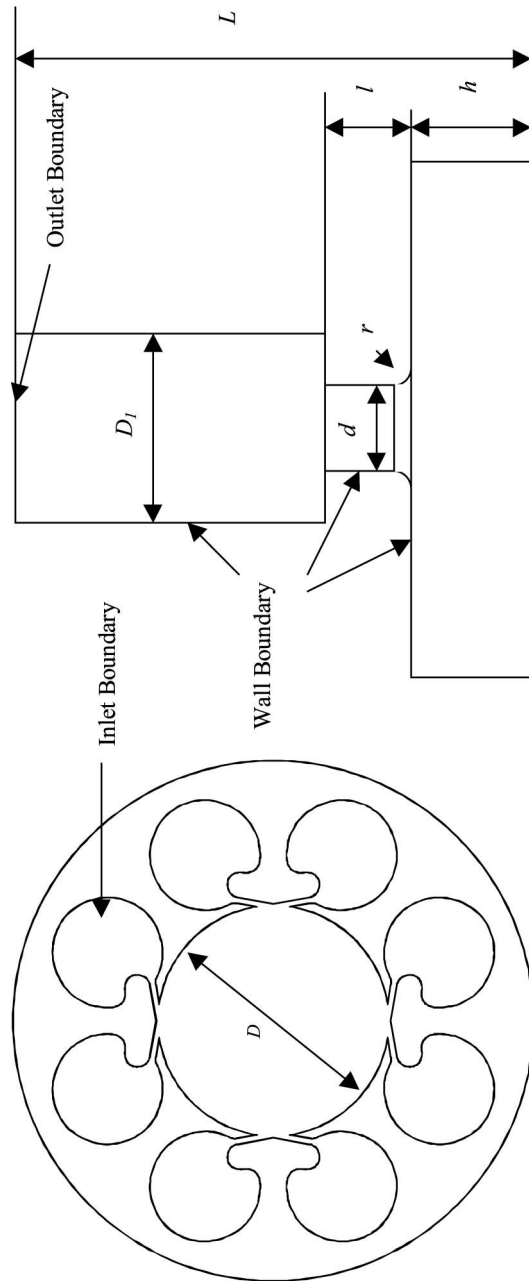


**Figure 1.**  
Illustration of the  
configuration and the  
boundary conditions for  
the eight port STuVA

---

This paper focuses on modelling the strongly swirling vortex flow state of the STuVA. Such a three dimensional swirling flow or a flow with very large curvature of streamlines is a classic problem of fluid mechanics. A considerable amount of literature on numerical simulation of swirling flows exists on cyclones (Slack *et al.*, 2000; He *et al.*, 1999; Malhotra *et al.*, 1994), combustors (Zhou and Chen, 2001; Zhou and Li, 2000) and swirling flames (Snegirev *et al.*, 2004; Battaglia *et al.*, 2000). A difficulty associated with solving such swirling flows is that the eddy-viscosity models fail to capture the anisotropy of strain and Reynolds stresses under the action of Coriolis and centrifugal forces. A strongly swirling flow tends to make a motion highly anisotropic, with a resistance to radial flow much higher than axial flow. It has been confirmed (Slack *et al.*, 2000; He *et al.*, 1999; Malhotra *et al.*, 1994; Snegirev *et al.*, 2004; Battaglia *et al.*, 2000) that the standard  $k-\varepsilon$  turbulent model is not suitable for simulation of the highly swirling flows. The algebraic stress model (ASM) is an economical way of accounting for the anisotropy of Reynolds stress without having to solve the full Reynolds stress transport equations. Fu and Qian (2002) and Rumsey *et al.* (2000) reported their computations of curvature flows in U-type ducts. However, a number of studies (Fu and Qian, 2002; Rumsey *et al.*, 2000; Speziale *et al.*, 2000; Jakirlic *et al.*, 2002) showed that the ASM assumptions cause loss of swirl-related curvature terms and are still insufficient to capture turbulent physics of swirling flows. Thus, it is recommended that for such swirling flows more advanced turbulence models, such as the RSM or the large eddy simulation (LES) for turbulent transport (Slack *et al.*, 2000; Holzapfel, 2004) should be employed.

The RSM provides information of all the stress components and contains exact terms for swirling effects in its stress transport equations, so it is capable of capturing most of the physical phenomena. A number of studies (Fu and Qian, 2002; Rumsey *et al.*, 2000; Speziale *et al.*, 2000; Jakirlic *et al.*, 2002; Holzapfel, 2004; Yang *et al.*, 1991) have confirmed that the RSM produced better results than the two equation models for swirling flows. However, the superiority of the RSM used for swirling flows is sometimes overemphasized. While it is true that the RSM is superior to the  $k-\varepsilon$  model for strongly swirling flows, one should not forget that the pressure-strain term is an isotropic assumption in the standard RSM. Although some high order correlation of the pressure-strain have been suggested, they need to be confirmed further for engineering applications. Recent studies (Jakirlic *et al.*, 2002) have shown that a negative sign of shear stresses was in contradiction with the experimental data. Furthermore, the dissipation rate equation in the RSM is still employed, which has no explicitly swirling terms that account directly for swirling. For high swirl rate, the RSM is still not sufficient to account for the anisotropies of the dissipation and strain. Moreover, complex engineering flows can be oblique to their grid, producing truncation errors and false diffusion in the direction normal to the flow, as well as in the stream-wise direction. Thus, the second order upwind or the third order QUICK schemes need to be employed to obtain an acceptable result. Thus, it is possible that for some industrial applications, the RSM can be too time-consuming, particularly for complex geometry there are convergence problems. The LES needs more computing resource than the RSM. Furthermore, the LES is still in development and applications to any realistic geometry are not viable despite significant progress (Holzapfel, 2004). Hence, for the sake of computational economy, this approach is still too expensive for industrial applications.

It is well-known that in the classic  $k-\varepsilon$  turbulent models, the normal Reynolds stresses are assumed to be in the equality. The isotropic character of the normal stresses is a consequence of the Kolmogorov assumption that the principal axes of the Reynolds stress tensor are parallel to the principal axes of the mean strain rate tensor. The coefficients of proportionality of the principal values are determined by a scalar quantity, which, in turn, can be obtained from two scalar transport equations. This assumption becomes particularly questionable if the mean streamlines have large curvatures like the flow within the STuVA. To improve accuracy of modelling for swirling flows, the  $k-\varepsilon$  model must be modified. Recent studies (He *et al.*, 1999; Malhotra *et al.*, 1994; Hsieh and Rajamani, 1991; Launder *et al.*, 1977) have indicated that after proper modification, the  $k-\varepsilon$  model can have the potential to be used for strongly swirling flows. Launder *et al.* (1977) introduced a Richardson number and an empirical coefficient in the dissipation equation used for the curvature correction. He *et al.* (1999) used the same approach to simulate the flow in a cyclone where a curvature correction term with a single empirical constant was added into the dissipation equation. Snegirev *et al.* (2004) modified the eddy viscosity coefficient to use a formula with Richardson number instead of the standard one. Launder *et al.* (1977) indicated that it might have been better to have made the curvature correction on the production term of the  $\varepsilon$ -equation as well as on the destruction part. Malhotra *et al.* (1994) just used this approach in which the expressions of both the production and destruction terms were altered together. These modifications of the production, destruction or both have been used successfully for the simulation of swirling or curved flows. In spite of numerous successes these modified  $k-\varepsilon$  models are not as widely validated as the standard  $k-\varepsilon$  models and have reduced popularity and generality. To date there is no generic turbulence model applicable to wide ranging industrial applications. Closure coefficients are a choice of the developer (Wilcox, 2002) so that models are optimised for specific applications.

In the standard  $k-\varepsilon$  models the standard values of the model constants were obtained using the experimental data from simple flat plate shear flows (Launder and Spalding, 1972) so it is not surprising that the conventional  $k-\varepsilon$  model with the standard values of the model constants produces unrealistic solutions for strong swirl flows in complex geometries. There are two basic approaches to modify the production and destruction terms for the curvature corrections in the standard  $k-\varepsilon$  model: the re-formalization of the production and destruction terms and the constant adjustments before the terms. It should be mentioned that both approaches have same the physical grounding, based on the curvature correction of the production and destruction terms. The term formalization approach has been widely studied (Slack *et al.*, 2000; He *et al.*, 1999; Malhotra *et al.*, 1994; Snegirev *et al.*, 2004). However, there are three drawbacks in the re-formalization approaches. Firstly, the success is achieved at the cost of loss of generality. Secondly, the re-formalisation must modify the codes, which may be impractical in many industrial applications. Thirdly, the swirl acts not only on the production and destruction terms but also the eddy viscosity. This cannot be corrected through the correction of the production and destruction terms.

The adjustment of the model constants is based on the fact that the model constants affect the eddy viscosity, and the production and destruction of dissipation rate of the turbulent kinetic energy. The modifications of the eddy viscosity, and the production and destruction of the dissipation rate make the Reynolds stresses and eddy viscosity

corrected. Thus, the anisotropic swirl flows can be corrected. However, there are few reports and no clear guidelines about how to adjust these constants although there is a certain physical background. A regulation how to adjust model constants has not yet emerged for 3D swirling flows.

The aim of this paper is to model the strongly swirling flows within the 8-port STuVA through which a better understanding of the complicated flow field can be achieved and useful guidelines drawn for its design. Another aim is to examine the performance of the conventional turbulent models in the complex engineering flows, and to explore approaches and the possibility to simulate the complex flow using the conventional two equation  $k-\varepsilon$  model by modifying their model constants. Furthermore, the physical mechanism of the model constants are studied and explained, with the aim of producing guidance on how to adjust model constants.

## 2. Experimental characterisation of the STuVA

A previously optimised (Priestman and Tippetts, 2000) design of eight port STuVA was characterised to provide basic data for comparison with the model predictions. The STuVA geometry is shown in Figure 1 with Table I giving details of the critical dimensions in millimetres. The axial outlet nozzle was made of brass and its 13 mm diameter section was 12 mm long. The inlet ports were 2.35 mm wide across the full chamber height.

A fan was used to draw air through the device from atmosphere. As the four tangential control ports were manifolded together these could be easily blocked such that the device operated in its minimum flow state. The pressure drop was measured using an inclined manometer on the outlet just downstream of the outlet nozzle. Pressure drop was limited to less than 20 cm of water to avoid compressibility effects. A rotameter positioned downstream of the outlet pressure tapping measured the flow rate, readings being adjusted for density. Pressure drop was measured to  $\pm 1$  millimetre of water. The rotameter accuracy was about  $\pm 2$  per cent.

## 3. Turbulence models

As the flow involves swirling, strongly accelerated, and re-circulating flows, it becomes necessary to use the conservation equations of mass and momentum in their full form.

### 3.1 Two equation model

The standard two-equation  $k-\varepsilon$  model (FLUENT, 1998; Versteeg and Malalasekera, 1995; Ferziger and Peric, 1999) is a semi-empirical turbulent model based on transport equations for the turbulent kinetic energy  $k$  and its dissipation rate  $\varepsilon$ , which are calculated from the following transport equations:

$$\rho \frac{Dk}{Dt} = \frac{\partial}{\partial x_i} \left( \left[ \mu + \frac{\mu_t}{\sigma_k} \right] \frac{\partial k}{\partial x_i} \right) - \overline{\rho u'_i u'_j} \frac{\partial u_j}{\partial x_i} + \beta g_i \frac{\mu_t}{Pr_t} \frac{\partial T}{\partial x_i} - \rho \varepsilon - 2\rho \varepsilon \frac{k}{\gamma RT} \quad (1)$$

Nozzle	$D$ (mm)	$D_1$ (mm)	$d$ (mm)	$h$ (mm)	$l$ (mm)	$L$ (mm)	$r$ (mm)
N8	90	50	13	29.1	20	149.1	4

**Table I.**  
Dimensions and  
parameters of STuVA

$$\rho \frac{D\varepsilon}{Dt} = \frac{\partial}{\partial x_i} \left( \left[ \mu + \frac{\mu_t}{\sigma_\varepsilon} \right] \frac{\partial \varepsilon}{\partial x_i} \right) + C_1 \frac{\varepsilon}{k} \left( -\overline{\rho u'_i u'_j} \frac{\partial u_j}{\partial x_i} + C_3 \beta g_i \frac{\mu_t}{Pr_t} \frac{\partial T}{\partial x_i} \right) - C_2 \rho \frac{\varepsilon^2}{k} \quad (2)$$

The turbulent viscosity is related to  $k$  and  $\varepsilon$  by:

$$\mu_t = \rho C_\mu \frac{k^2}{\varepsilon} \quad (3)$$

The above equations contain six adjustable constants  $C_\mu$ ,  $C_1$ ,  $C_2$ ,  $C_3$ ,  $\sigma_k$  and  $\sigma_\varepsilon$ . The standard values of the model constants in the standard  $k$ - $\varepsilon$  model are 0.09, 1.44, 1.92, 2.0, 1.0 and 1.3, respectively, (FLUENT, 1998; Versteeg and Malalasekera, 1995; Ferziger and Peric, 1999).

### 3.2 Reynolds stress models (RSM)

The standard RSM can be given as following (FLUENT, 1998; Versteeg and Malalasekera, 1995; Ferziger and Peric, 1999):

$$\frac{DR_{ij}}{Dt} = P_{ij} + D_{ij} - \varepsilon_{ij} + \Pi_{ij} + \Omega_{ij} \quad (4)$$

where  $R_{ij} = \overline{u'_i u'_j}$ :

$$P_{ij} = - \left( R_{im} \frac{\partial u_j}{\partial x_m} + R_{jm} \frac{\partial u_i}{\partial x_m} \right) \quad (5)$$

$$D_{ij} = \frac{\partial}{\partial x_m} \left( C_\mu \frac{k^2}{\varepsilon \sigma_k} \frac{\partial R_{ij}}{\partial x_m} \right) \quad (6)$$

$$\varepsilon_{ij} = \frac{2}{3} \varepsilon \delta_{ij} \quad (7)$$

$$\Pi_{ij} = -C_1 \frac{\varepsilon}{k} \left( R_{ij} - \frac{2}{3} k \delta_{ij} \right) - C_2 \left( P_{ij} - \frac{2}{3} P_{ij} \delta_{ij} \right) \quad (8)$$

$$\Omega_{ij} = -2\omega_k (R_{jm} e_{ikm} + R_{im} e_{jkm}) \quad (9)$$

$$\varepsilon_{ij} = \frac{\partial}{\partial x_m} \left( C_\mu \frac{k^2}{\varepsilon \sigma_\varepsilon} \frac{\partial \varepsilon_{ij}}{\partial x_m} \right) + 2k C_{1\varepsilon} C_\mu E_{ij} E_{ij} - C_{2\varepsilon} \frac{\varepsilon^2}{k} \quad (10)$$

Here  $\omega_k$  is the rotation vector and  $e_{ijk} = 1$  if  $i, j$  and  $k$  are different and in cyclic order;  $e_{ijk} = -1$  if  $i, j$  and  $k$  are different and in anti-cyclic order, and  $e_{ijk} = 0$  if any two indices are the same. The above equations contain seven adjustable constants  $C_\mu$ ,  $C_1$ ,  $C_2$ ,  $C_{1\varepsilon}$ ,  $C_{2\varepsilon}$ ,  $\sigma_k$  and  $\sigma_\varepsilon$ . The standard values of the model constants in the RSM model are 0.09, 1.8, 0.6, 1.44, 1.92, 1.0 and 1.3, respectively.

### 4. Near-wall models

It is well-known that turbulent flows are significantly affected by presence of walls. It is in the near-wall region that the solution variables change with large gradients, and the momentum and other scalar transports occur most vigorously. Therefore, an accurate representation of flows in the near-wall region is needed for accurate predictions of wall-bounded turbulent flows. The common near wall models are wall

functions, non-equilibrium wall functions and the two layer zonal model. The wall functions do not resolve viscosity affected inner regions (viscous sublayer and buffer layer). Instead, semi-empirical formulas are used to bridge the viscosity-affected regions between the wall and the fully-turbulent region. Non-equilibrium functions assume that the wall-neighbouring cells consist of a viscous sub-layer and a fully turbulent layer which need to resolve the  $k$  equation at the wall-neighbouring cells. Thus, the non-equilibrium wall functions partly account for non-equilibrium effects neglected in the standard wall function. The two layer near-wall models divide the whole domain into two regions, a viscosity-affected region and a fully-turbulent region. The turbulent models are modified to enable the viscosity-affected region to be resolved with a refined mesh close to the wall. Recent studies (Wang *et al.*, n.d.) have found that the two-layer model is more suitable for simulation of STuVA geometry. Hence, it is also used in the work reported here.

In the two-layer model, the demarcation of the viscosity-affected region and the fully-turbulent region is determined by a wall-distance-based turbulent Reynolds number,  $Re_y$ , defined as:

$$Re_y \equiv \frac{\rho y \sqrt{k}}{\mu} \quad (11)$$

where  $y$  is the normal distance from the wall at the cell centres. When  $Re_y < 200$ , the flow is in the viscosity-affected near-wall region. When  $Re_y > 200$ , the flow is in the fully turbulent region.

## 5. Numerical considerations

The computer program used in the present work was the FLUENT package. The code is able to accommodate non-uniform and unstructured grids. In the present studies the unstructured tetrahedral grids are automatically generated by the GAMBIT, as shown in Figure 2.

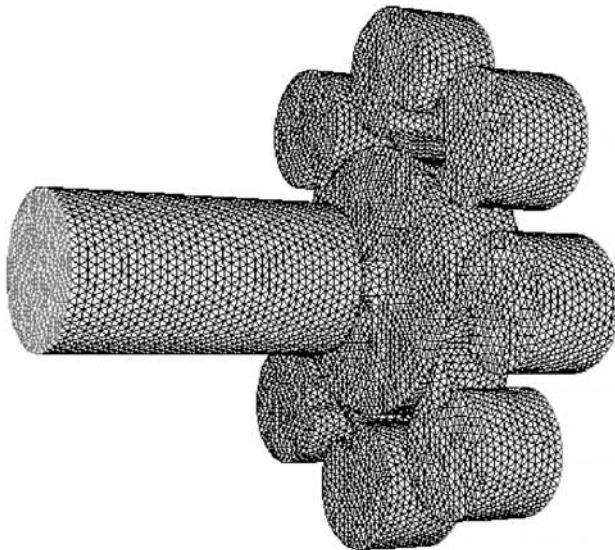


**Figure 2.**  
Geometry and tetrahedral  
mesh of the eight port  
STuVA



Numerical tests were performed in order to assess effect of mesh sizes on the solutions. The unstructured tetrahedral mesh with 0.148, 0.285, 0.535 and 1.23 million cells were used for the tests. It was found that the difference of the solutions was of the order of 12 per cent or less between 0.148 and 1.23 million cells for the first order upwind scheme and 5.5 per cent or less for the QUICK scheme using the  $k-\epsilon$  model. The difference of the solutions was 2.6 per cent between 0.535 and 1.23 million cells for the first order upwind scheme and 1.2 per cent for the QUICK scheme using the  $k-\epsilon$  model. All the computations started using the mesh of 0.535 million cells. As the viscosity-affected region requires being resolved for the two layer near-wall mode, the near-wall cells were refined in terms of  $y^+$  after several hundred iterations.  $y^+$  is a distance from the wall at the wall-adjacent cells, defined as  $\rho u_t y / \mu$ . Where  $u_t$  is the friction velocity,  $\mu$  is dynamic viscosity of the fluid and  $y$  is a distance away from the nearest wall. The mesh refinement was made in the FLUENT in terms of  $y^+$  on the order of  $y^+ = 1$ . A locally refined mesh near-wall region is shown in Figure 3. The final mesh used for all the computations was 0.844 million cells. It was found that the difference of the solutions from its consecutive grid of 1.23 million cells was 2.4 per cent for the first order upwind scheme and 0.66 per cent for the QUICK scheme. This is seen as acceptable in industrial applications.

Since the governing partial differential equations are elliptic, it is necessary to define boundary conditions for all variables on all boundaries of the flow domain. Three types of boundary conditions were used, inlet, outlet and wall, as shown in Figure 1. The boundaries where steady-state conditions should be specified are the inlets and outlet. The pressure at the inlets and outlet were pre-set the beginning of the computation to correspond to the measured pressure drop across the device. The predicted overall flowrate through the device could then be compared with the

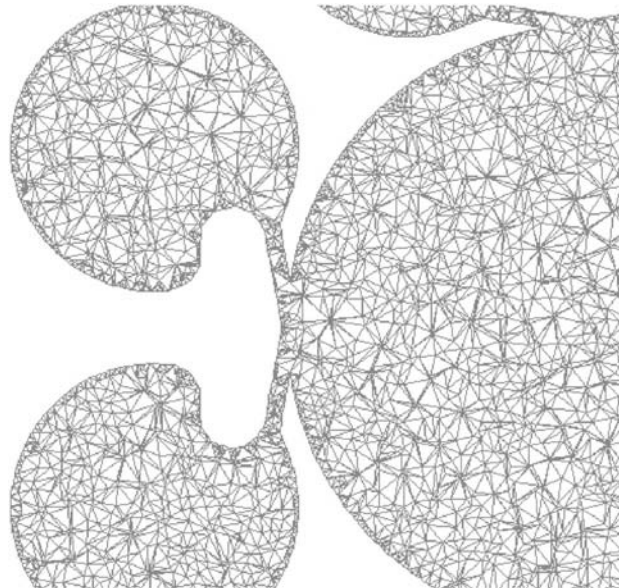


**Figure 3.**  
Locally refined cells at the  
near walls using  $y^+ = 1$

measured one. At the solid wall, the usual non-slip condition was applied, hence the velocities at the walls were specified to be zero.

## 6. Results and discussions

### 6.1 Modelling with the standard model constants

Figure 4 shows the measured flowrates, expressed as an average outlet velocity, with values predicted using the  $k-\epsilon$  model and the RSM with the standard values of the model constants, for the same pressure drop. The computations with the first order upwind scheme used the two layer near-wall model. For the QUICK scheme, the wall function models were used. For the RSM, the QUICK scheme was only used for the momentum and Reynolds stress equations, with the first order upwind for others. It is apparent that the predicted flow rates are more than double the measured values. For the two equation  $k-\epsilon$  models, the turbulent transport equations, particularly the dissipation rate equation, are empirical approximations of the actual equations. In reality, the  $\epsilon$ -equation itself is very much a black-box and cannot represent turbulent physics. Hence, it can be expected to have a poor behaviour for the simulation of such strongly swirling flows. Using the RSM with the QUICK scheme gives the smallest over-prediction, but it is still severe. Further refinement of the cells and using high order schemes for all the equations may be able to further reduce these errors, but convergence difficulties can be encountered. The computation using a combination of the RSM and the QUICK is also very expensive. Generally speaking, the CPU time

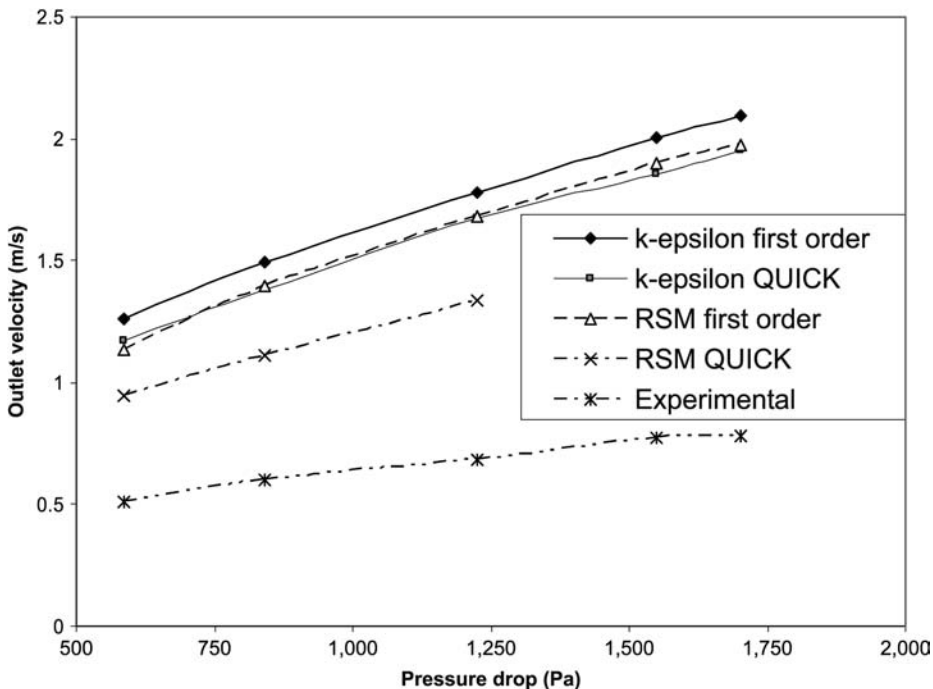


**Figure 4.** Comparison between the  $k-\epsilon$  and RSM models with standard constants and experimental data

using QUICK was about twice that for the first order scheme for the same turbulence models, and the time taken with the RSM was about ten times that with the  $k-\varepsilon$  model. Hence, computational economy is taken into account, the standard  $k-\varepsilon$  model is still comparable.

6.2 Modelling with the adjustment of the model constants

The influence of model constants on the computational results were initially evaluated using the standard  $k-\varepsilon$  model with the first order upwind scheme and the two layer near-wall model. The near-wall mesh was locally refined using  $y^+ = 1$  to improve the accuracy.

We note that from equations (1) and (2), that when buoyancy effects are neglected the third terms on the right hand side vanish. Hence, we do not need to consider  $C_3$ . In equation (2),  $C_1$  represents the fraction of production in the  $\varepsilon$ -equation and  $C_2$ , the fraction of the destruction.  $C_\mu$  is the fraction of the eddy viscosity which represents the turbulent viscosity. Prandtl numbers  $\sigma_k$  and  $\sigma_\varepsilon$  connect the diffusion of  $k$  and  $\varepsilon$  to the eddy viscosity  $\mu_t$ . The effects of the two Prandtl numbers can be combined to those of  $\mu_t$  or  $C_\mu$  since  $u_t/\sigma$  is proportional to  $C_\mu/\sigma$ . Thus, only the three constants,  $C_\mu$ ,  $C_1$  and  $C_2$  are considered here. The ranges of adjustment of the model constants are given in Table II.

Figure 5 shows the influence of changing  $C_2$  on the solutions with  $C_\mu = 0.09$  and  $C_1 = 1.44$ , their standard values. The predicted flow rate is seen to decrease with increasing  $C_2$ , but only when  $C_2$  reaches an unrealistically high value of 70, the predicted outlet velocity falls to the measured value. For predictions with  $C_\mu = 0.9$  and  $C_1 = 1.0$ , as shown in Figure 6,  $C_2 = 0.6$  is close to the data. We note that the dissipation rate  $\varepsilon$  of the turbulent kinetic energy due to work done by the smallest eddies against viscous stress decreases as the dissipation destruction increases in equation (2). Thus, the destruction term in the  $k$ -equation decreases and the turbulent kinetic energy  $k$  increases in equation (1). This leads to an increase of the eddy viscosity in equation (3), the flow resistance increases and the flow rate falls.

The effects of  $C_1$  on the outlet velocity are given in Table III for a pressure drop of 841 Pa and  $C_\mu = 0.09$  and  $C_2 = 1.92$ , their standard values. Even when  $C_1 \leq 0.001$ , the flow rate has not fallen significantly. The effect of the production term in  $\varepsilon$ -equation on the solution becomes less and less with decreasing  $C_1$ . The decrease of the production in the  $\varepsilon$ -equation causes a decrease of the turbulent dissipation rate  $\varepsilon$ , and so turbulent kinetic energy  $k$  increases. The increase of  $k$  and the decrease of  $\varepsilon$  lead to the increase of the eddy viscosity in equation (3), reducing the flowrate.

Although if any one of  $C_\mu$ ,  $C_1$  and  $C_2$  is adjusted the predicted results can be improved, a better approach is to adjust the three model constants together. Figures 6 and 7 show that when  $C_\mu$ ,  $C_1$  and  $C_2$  are adjusted the predictions approach the data more quickly. Of course care should be taken that the adjustments of model constants

**Table II.**  
The arrange of five adjustable constants

Model constants	$C_\mu$	$C_1$	$C_2$	$\sigma_\varepsilon$	$\sigma_k$
The standard value	0.09	1.44	1.92	1.30	1.00
Range	0.09 ~ 60	0.0 ~ 1.5	0.50 ~ 80	1.30	1.00

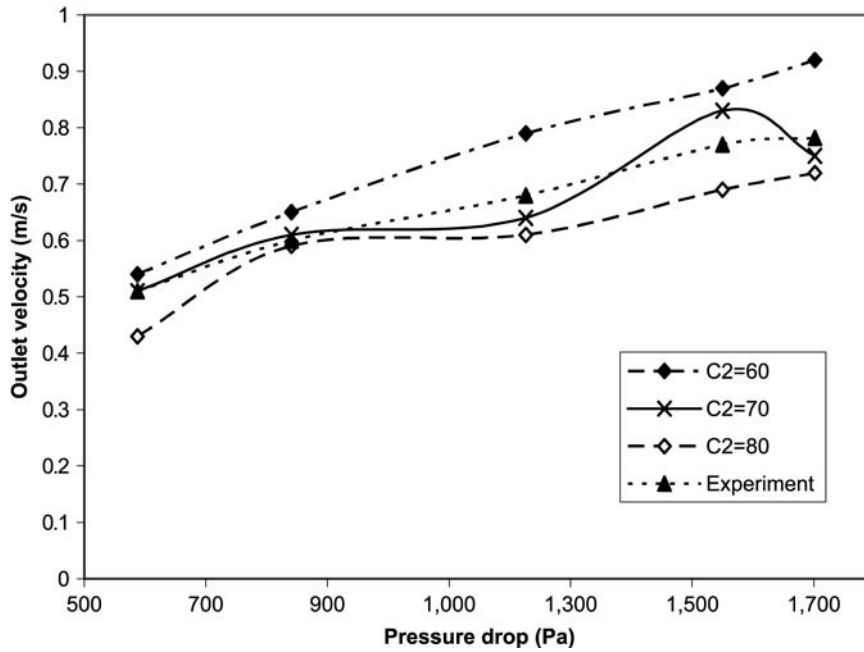


Figure 5. The effect of  $C_2$  on the solutions when  $C_\mu = 0.09$  and  $C_1 = 1.44$

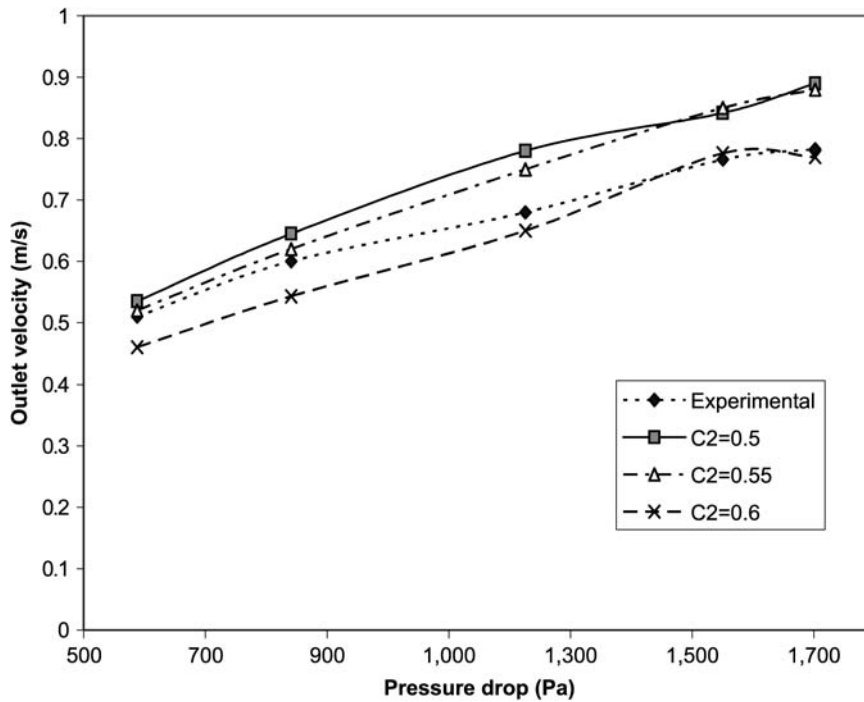


Figure 6. The effect of  $C_2$  on the solutions when  $C_\mu = 0.9$  and  $C_1 = 1.0$

are not too large, which could lead to a physically unrealistic solution. Figure 8 shows a physically unrealistic flow field produced by too large adjustments of  $C_\mu$ ,  $C_1$  and  $C_2$  to 0.9, 1.0 and 6.0, respectively. It can be seen that after the fluid enters the vortex chamber, there is nearly no swirling flow or the swirling flow becomes very weak and the fluid flows directly to the central nozzle. The improper adjustment of the model constants has resulted in a too large an eddy viscosity or Reynolds stresses. Thus, the fluid becomes non-Newton's with stresses nonlinearly related to the strain.

As mentioned in the introduction, if only model constants were adjusted, the solution could be improved but this may be insufficient. Hence, one should pay attention to the numerical errors. Numerical diffusion can cause substantial errors for such a three dimensional flow, a high order scheme should be used. Using the QUICK scheme, the same accuracy results can be obtained by adjusting a small amount of the model constants. Figure 7 shows relatively good agreement between the predictions and experimental data when  $C_\mu$ ,  $C_1$  and  $C_2$  are 0.09, 1.2 and 2.0, respectively, very close to their standard values. The corresponding flow fields are shown in Figure 9. It can be seen that the swirl intensification increases with increasing inlet pressure.

Table III.

$C_1$	1.44	1.2	0.3	0.1	0.05	0.001	0.0001	0.0	Exp
Outlet velocity	1.82	1.52	1.32	1.28	1.27	1.26	1.26	1.26	0.60

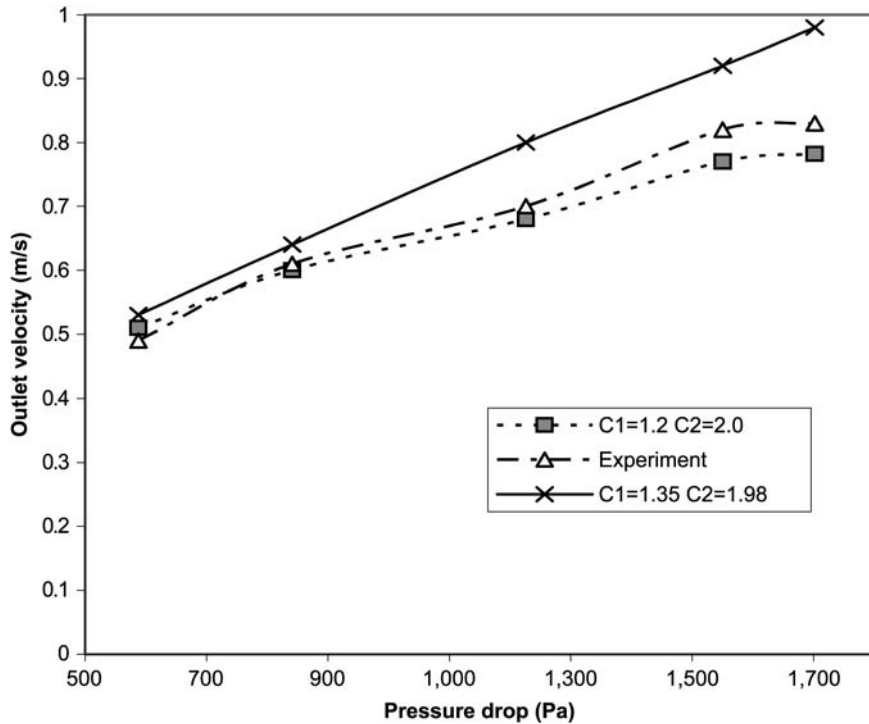
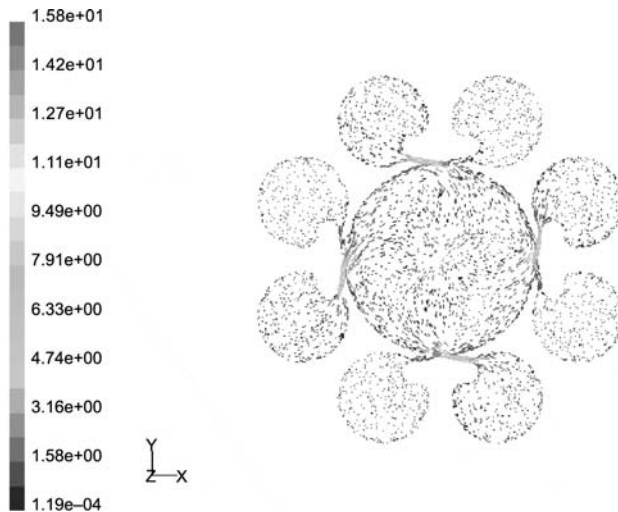


Figure 7.  
A comparison between experimental data and predicted results using the QUICK scheme when  $C_\mu = 0.09$



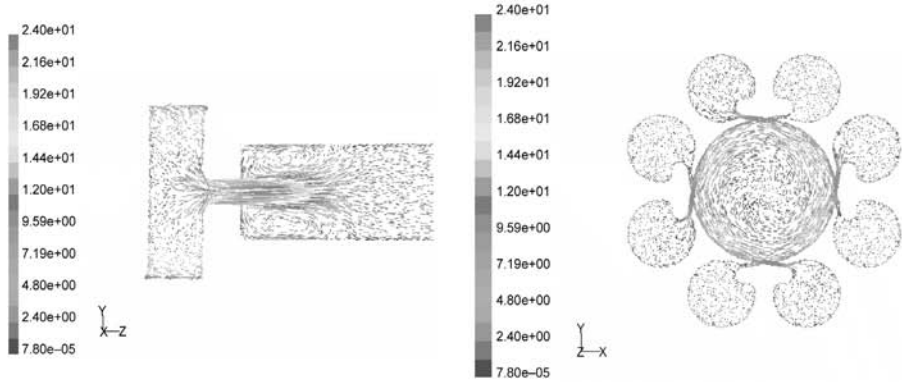
**Figure 8.**  
An unrealistic flow field  
resulting from too large an  
adjustment of the model  
constants (inlet  
pressure = 1,226 (Pa))

The above indicates that the eddy viscosity  $\mu_t$  increases as  $C_\mu$  and  $C_2$  increase and as  $C_1$  decreases. However, there is the risk of producing a physically unrealistic flow field if the adjustments are too large. The best way to adjust the model constants is to consider  $C_1$  and  $C_2$  together since they are dependent on each other. A proper degree of the adjustment is that the ratio of  $C_1$  to  $C_2$  is in range  $0.55 \sim 0.85$ . Then a slight adjustment of  $C_\mu$  is sufficient to obtain a reasonable flow field. Figures 7 and 9 show that when all the model constants are close to their standard values, a slight adjustment can model a very strongly swirling flow when using the QUICK scheme. Compared to the results in Figure 4, a slight adjustment of the model constants does improve greatly the modelling accuracy.

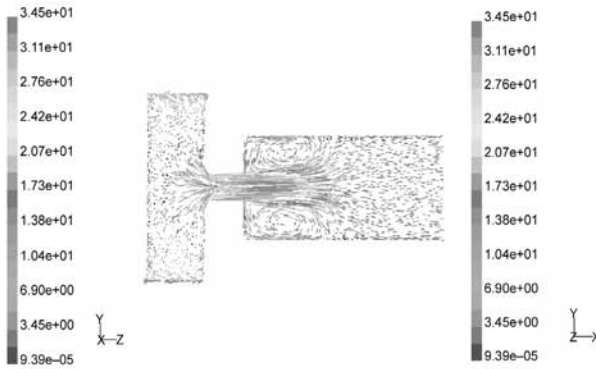
The direct effect of the swirling flow on the model is combined into these empirical model coefficients. It may be argued that if the modified constants can be applied to other cases then the approach is useful and reasonable. It is desirable to have a set of general model constants. However, a set of general constants does not exist because of the inherent limitation of the  $k-\varepsilon$  model. Alternatively one can explore the regularity or the trend of the effect of the model constants on the solutions. The numerical results do show that the errors are greatly improved by adjusting the model constants based on the eddy viscosity and the production and destruction of  $k$  and  $\varepsilon$ . The dissipation rate  $\varepsilon$  of the turbulent kinetic energy caused by work done by the smallest eddies against viscous stress decreases as the dissipation destruction constant  $C_2$  increases or the dissipation production constant  $C_1$  decreases in equation (2). Thus, the destruction term in  $k$ -equation decreases and the turbulent kinetic energy  $k$  increases in equation (1), which overall leads to an increase of the eddy viscosity in equation (3).

## 7. Conclusions

A numerical procedure has been performed using semi-empirical treatments for the strongly swirling three dimensional flow within a STuVA. The standard two-equation  $k-\varepsilon$  model and the RSM with the two layer near-wall model were employed. The computations confirm that the more costly RSM has an advantage over the  $k-\varepsilon$  models



(a) Inlet pressure = 587.7 (Pa)



(b) Inlet pressure = 1226 (Pa)

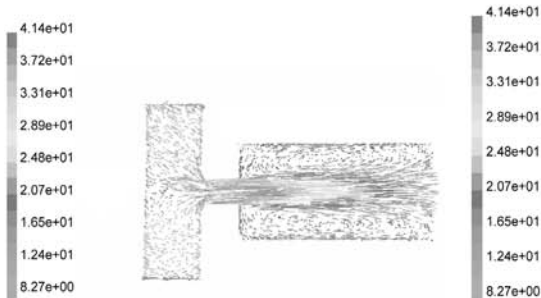


**Figure 9.** Flow fields of the eight port STuVA using QUICK scheme: (a) inlet pressure = 587.7 (Pa); (b) inlet pressure = 1,226 (Pa); (c) inlet pressure = 1,550 (Pa)

for swirling flows due to the explicitly appearance of rotation or swirling terms in the transport equations. However, for very strongly swirling flows, the standard RSM severely over-predicted the flow rate even using the QUICK scheme. The error may result from the assumption of the pressure-strain terms and isotropic calculation of  $\varepsilon$  equation. Also convergence difficulties were encountered when using a combination of the RSM and the QUICK scheme. Hence, overall, the RSM may have less advantage over the conventional  $k$ - $\varepsilon$  model for strongly swirling flows, since it must be modified like the conventional  $k$ - $\varepsilon$  model.

The adjustment of model constants can be interpreted as making modifications to the eddy viscosity, and to the production and destruction terms of the  $\varepsilon$ -transport equation. An increase of  $C_\mu$  directly increases the eddy viscosity and Reynolds stresses. The eddy viscosity and Reynolds stresses decrease as  $C_2$  decreases or  $C_1$  increases. The relationship between the model constants and the eddy viscosity and Reynolds stresses determines how the model constants affect the solution. A proper degree of the adjustment of model constants is that the ratio of  $C_1$  to  $C_2$  is in range 0.55 ~ 0.85. Then a slight adjustment of  $C_\mu$  is sufficient to obtain a reasonable flow field for very strongly swirling flows using the conventional  $k$ - $\varepsilon$  model with the QUICK scheme. Such adjustments of the constants could be a simple and useful approach for various industrial applications. Although further work is required for other industrial cases, considering the complex of re-formulation approaches in industrial applications the present approach is encouraging.

## References

- Battaglia, F., Rehm, R.G. and Baum, H.R. (2000), "The fluid mechanics of fire whirls: an inviscid model", *Physics of Fluids*, Vol. 12 No. 11, pp. 2859-67.
- Ferziger, J.H. and Peric, M. (1999), *Computational Methods for Fluid Dynamics*, 2nd ed., Springer, New York, NY.
- FLUENT (1998), *FLUENT5 User's Guide*, Vol. 2, Fluent Inc., Lebanon, NH, July.
- Fu, S. and Qian, W.Q. (2002), "Development of curvature sensitive nonlinear eddy-viscosity model", *AIAA Journal*, Vol. 40 No. 11, pp. 2225-33.
- He, P., Salcudean, M. and Gartshore, I.S. (1999), "A numerical simulation of hydrocyclones", *Trans IChemE, Part A*, Vol. 77, pp. 429-41.
- Holzappel, F. (2004), "Adjustment of subgrid-scale parameterizations to strong streamline curvature", *AIAA Journal*, Vol. 42 No. 7, pp. 1369-77.
- Hsieh, K.T. and Rajamani, R.K. (1991), "Mathematical model of the hydrocyclone based on physics of fluid flow", *AIChE J.*, Vol. 37 No. 5, pp. 735-46.
- Jakirlic, S., Hanjalic, K. and Tropea, C. (2002), "Modeling rotating and swirling turbulent flows: a perpetual challenge", *AIAA Journal*, Vol. 40 No. 10, pp. 1984-96.
- Lauder, B.E., Priddin, C.H. and Sharma, B.I. (1977), "The calculation of turbulent boundary layers on spinning and curved surfaces", *ASME J. of Fluids Engineering*, Vol. 99, pp. 231-9.
- Lauder, B.E. and Spalding, D.B. (1972), *Lectures in Mathematical Models of Turbulence*, Academic Press, London.
- Malhotra, A., Branion, R.M.R. and Hauptmann, E.G. (1994), "Modelling the flow in a hydrocyclone", *Canad. J. Chem Eng.*, Vol. 72, pp. 953-60.



- Priestman, G.H. and Tippetts, J.R. (1984), "Development and potential of power fluidics for process flow control", *Transactions of the Institution of Chemical Engineers, Part A*, Vol. 62 No. 2, pp. 67-80.
- Priestman, G.H. and Tippetts, J.R. (1998), "The application of power fluidics to level control in multiphase separators", BHR Group Multiphase Technology, pp. 119-29.
- Priestman, G.H. and Tippetts, J.R. (2000), "Fluidic level control in gas-liquid separators", *Trans. of the Institution of Chemical Engineers, Part A*, Vol. 78, A5, pp. 690-7.
- Priestman, G.H. and Tippetts, J.R. (2002), Fluidic Level Control Systems, United States Patent US 6,402,820 B1, June.
- Rumsey, C.L., Gatski, T.B. and Morrison, J.H. (2000), "Turbulence model predictions of strongly curved flow in a U duct", *AIAA Journal*, Vol. 38 No. 8, pp. 1394-402.
- Slack, M.D., Prasad, R.O., Bakker, A. and Boysan, F. (2000), "Advances in cyclone modelling using unstructured grids", *Trans. IChemE, Part A*, Vol. 78, pp. 1098-104.
- Snegirev, A.Yu., Marsden, J.A., Francis, J. and Makhviladze, G.M. (2004), "Numerical studies and experimental observations of whirling flames", *Int. J. of Heat and Mass Transfer*, Vol. 47, pp. 2523-39.
- Speziale, C.G., Younis, B.A. and Berger, S.A. (2000), "Analysis and modelling of turbulent flow in an axially rotating pipe", *J. of Fluid Mechanics*, Vol. 407, pp. 1-26.
- Versteeg, H.K. and Malalasekera, W. (1995), *An Introduction to Computational Fluid Dynamics: The Finite Volume Method*, Longman Scientific & Technical, London.
- Wang, H., Beck, S.B.M., Priestman, G.H. and Boucher, R.F. (1997), "Fluidic pressure pulse transmitting flow meter", *Transactions of the Institution of Chemical Engineers, Part A*, Vol. 75, A4, pp. 381-91.
- Wang, J., Priestman, G.H. and Tippetts, J.R. (n.d.), An Assessment of turbulence and near-wall models applied to the simulation of a symmetrical turn-up vortex amplifier (submitted).
- Wilcox, D.C. (2002), *Turbulence Modelling for CFD*, 2nd ed., DCW Industries, Inc., La Cañada, CA.
- Yang, Z.Y., Priestman, G.H. and Boysan, H.F. (1991), "Internal flow modelling of vortex throttles", *Proceedings of Institute of Mechanical Engineers, Part C, J. of Mechanical Engineering Science*, Vol. 205, pp. 405-13.
- Zhou, L.X. and Chen, T. (2001), "Simulation of swirl gas-particle flows using USM and k-ε-kp two-phase turbulence models", *Powder Technology*, Vol. 114, pp. 1-11.
- Zhou, L.X. and Li, Y. (2000), "Simulation of swirl gas-particle flows using a DSM-PDF two-phase turbulence model", *Powder Technology*, Vol. 113, pp. 70-9.

**Corresponding author**

Junye Wang can be contacted at: [j.wang3@lboro.ac.uk](mailto:j.wang3@lboro.ac.uk)